

---

# 000 SINGER: LEVERAGING SEMANTIC IDENTIFIER HIER- 001 ARCHIES FOR GENERATIVE RECOMMENDATION 002

003 **Anonymous authors**  
004

005 Paper under double-blind review  
006

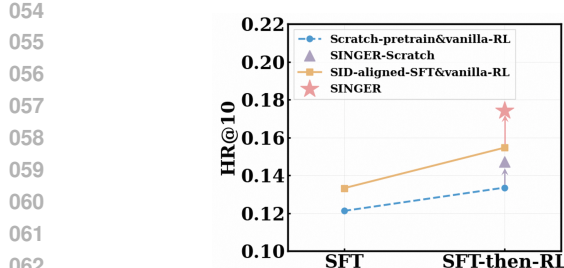
## 007 ABSTRACT 008

009 Recent advances in large language models (LLMs) have sparked a new line of  
010 generative recommendation, where the recommender autoregressively generates a  
011 sequence of Semantic IDs (IDs)—item identifiers in the SID space—rather than  
012 ranking a pre-selected candidate set of item titles in the language space. Although  
013 the current Supervised Fine-Tuning followed by Reinforcement Learning (SFT-  
014 then-RL) pipeline improves performance, it still fails to adequately model the SID  
015 space. Specifically, (i) SFT often leads to superficial SID understanding by merely  
016 forcing memorization of a closed SID vocabulary, and (ii) rule-based RL typically  
017 relies on coarse-grained rewards that treat all incorrect IDs equally, regardless of  
018 their hardness. To address these challenges, we propose *SID-Navigated GEnerative*  
019 *Recommender (SINGER)*, a framework that integrates fine-grained SID knowledge  
020 throughout training. SINGER comprises two components: (1) Full-Process SID  
021 Alignment, which embeds alignment objectives throughout both SFT and RL  
022 to strengthen the model’s understanding of the SID space; (2) SID-Navigated  
023 Reinforcement Learning, which consists of SID-level rewards that grade each  
024 trajectory by the deepest correctly matched SID layer, together with a SID-prefix  
025 curriculum sampling strategy that supplies partial prefixes as intermediate guidance  
026 for hard cases. Experiments on public benchmarks demonstrate that SINGER  
027 consistently outperforms strong sequential, generative, and recent LLM-based  
028 baselines across standard metrics, validating the benefit of integrating hierarchical  
029 SID signals with the world knowledge of pretrained LLMs.  
030

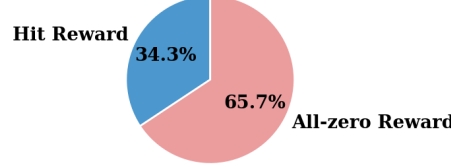
## 031 1 INTRODUCTION 032

033 The powerful sequence modeling capabilities of large language models (LLMs) have enabled their  
034 adaptation to recommender systems (Bao et al., 2023; Sheng et al., 2024; Hu et al., 2025; He et al.,  
035 2025a; Wu et al., 2024; Fang et al., 2020), with generative recommendation emerging as a promising  
036 direction that leverages autoregressive generation for item prediction (Rajput et al., 2023; Zheng et al.,  
037 2024; Qu et al., 2024; Zhai et al., 2024; Deng et al., 2025; Wang et al., 2025a). This paradigm centers  
038 on generating sequences of Semantic IDs (IDs)—discrete tokens that encode item semantics through  
039 quantization of continuous embeddings (Zeghidour et al., 2022; Luo et al., 2024). By promoting  
040 token sharing across semantically related items, SIDs facilitate efficient handling of large-scale  
041 catalogs while naturally aligning with the step-by-step (chain-of-thought) reasoning paradigm of  
042 LLMs (Rajput et al., 2023; Zeghidour et al., 2022; Luo et al., 2024; Deng et al., 2025; Singh et al.,  
043 2024).  
044

045 Upon scrutinizing prior studies on generative recommenders, we can summarize a common training  
046 pipeline: (1) Beginning with items’ textual descriptions or embeddings, a quantization method  
047 transforms continuous vectors into SIDs. (2) The model is then trained to generate these SIDs in  
048 an end-to-end manner, typically following two primary approaches: *scratch-trained recommenders*  
049 that train Transformer (Vaswani et al., 2017) from scratch on user interaction sequences (Rajput  
050 et al., 2023; Zhai et al., 2024; Deng et al., 2025; Wang et al., 2025a), and *SID-aligned Recommenders*  
051 that adapt pretrained LLMs from the language space into SID space through supervised fine-tuning  
052 (SFT) (Zheng et al., 2024; Qu et al., 2024). Although these methods achieve promising performance,  
053 the integration of reinforcement learning (RL) for deeper alignment with user interaction sequences  
remains relatively underexplored (Chen et al., 2024).



063 (a) Performance under Different Training  
064 Paradigms.  
065



(b) Sample hit reward distribution.  
069

070 Figure 1: Results on the Industrial dataset. Figure 1a illustrates the performance, with respect to  
071 HitRatio@10 under different training paradigms. Figure 1b shows the proportion of RL-sampled  
072 outputs from the SFT-initialized model that receive a non-zero reward.  
073  
074  
075  
076  
077  
078

Inspired by the recent success of the **SFT-then-RL** paradigm (Shao et al., 2024; Yoshihara et al., 2025; OpenAI et al., 2024), we aim to establish a generative recommendation framework that adapts this paradigm to the unique characteristics of recommendation tasks. Specifically, we first explore applying Group Relative Policy Optimization (GRPO) (DeepSeek-AI et al., 2025) after the initial SFT phase, considering both scratch-trained and SID-aligned recommenders. Our preliminary experiments (*cf.* Figure 1a) demonstrate the effectiveness of the SFT-then-GRPO paradigm in generative recommendation, consistently outperforming the SFT-only baselines. Building on this, we further investigate two critical limitations that arise when directly transferring the standard SFT-then-RL paradigm to recommendation, which constrain its full potential in this domain:

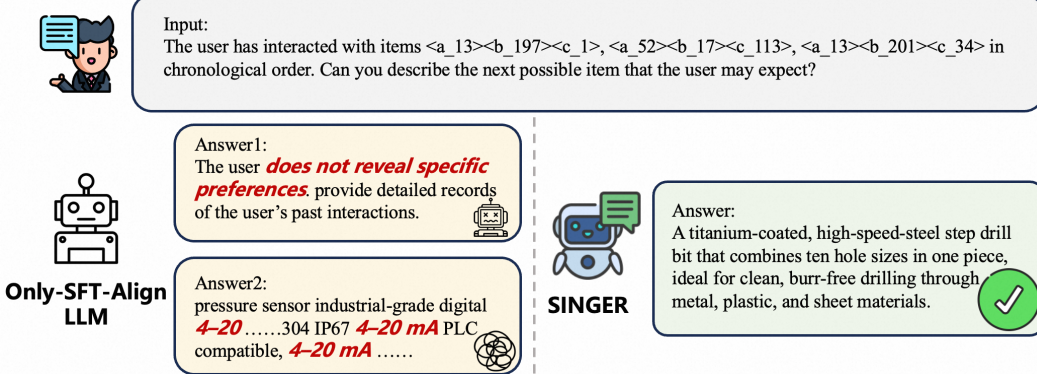
• **Limited SID Understanding in Alignment.** The SFT alignment process constrains LLMs to project outputs into a closed SID vocabulary through supervised training on user-item interaction sequences. Such rigid constraint mainly encourages superficial pattern matching rather than true semantic understanding of SIDs. As illustrated in Figure 2, even after SFT the model often fails to exploit SID histories correctly: it either resorts to generic responses citing insufficient user information, or produces lengthy, repetitive item descriptions indicative of collapsed generation. While the world knowledge in pretrained LLMs should be beneficial for understanding item semantics and user preference (*cf.* Figure 1a), the current alignment pipeline exploits it only superficially, highlighting the need for a more systematic approach that integrates SID understanding throughout the entire training process.

• **Ineffective Reward Assignment in RL.** The standard rule-based RL training treats each SID sequence as an indivisible unit—if any token in a generated sequence fails to match the ground-truth, the entire sequence is penalized with zero reward. This binary reward mechanism overlooks the rich relational structure among SIDs, unable to distinguish between near-correct and completely irrelevant predictions. The resulting sparse rewards (*cf.* Figure 1b) deprives the model of useful learning signals on hard cases—those rollouts that narrowly miss exact matches and thus receive zero advantages (Yu et al., 2025)—which represent the most critical cases for developing genuine reasoning capabilities over the SID taxonomy. Consequently, RL optimization tends to reinforce patterns already memorized during pre-training and SFT (Chu et al., 2025; Yue et al., 2025; Liu et al., 2025), rather than learning to navigate semantic relationships that would enable better performance on challenging cases.

To address the above limitations, we introduce *SID-Navigated GEnerative Recommenders (SINGER)*, a generative recommendation framework that enhances both SID comprehension and reward utilization throughout the SFT-then-RL process. SINGER is built on two key components:

• **Full-Process SID Alignment.** We embed a set of alignment objectives throughout the entire SFT-then-RL pipeline to achieve deeper SID alignment. Specifically, we integrate discrete SID tokens into the LLM’s vocabulary and introduce a series of auxiliary alignment tasks (*e.g.*, explicit item title to SID mapping) that are enforced during both SFT and RL phases. This ensures the model fully internalizes the structural semantics of SIDs.

108  
109  
110  
111  
112  
113  
114  
115  
116  
117  
118  
119  
120



121 Figure 2: Only-SFT-Align case study. The model is fed a SID-formatted interaction history and asked  
122 to describe the next item. The Only-SFT-Align LLM fails to interpret the SID tokens (Answer 1) or  
123 generates verbose, repetitive, and disordered text (Answer 2), underscoring the shallow alignment  
124 achieved by SFT alone. By contrast, SINGER correctly understands the SID sequence and produces  
125 a concise, coherent item description.

126

- 127 • **SID-Navigated Reinforcement Learning.** We develop a novel RL framework that leverages SID  
128 hierarchy to provide more informative learning signals:

129 (a) **SID-Prefix Curriculum Sampling.** Let the ground-truth item be a hierarchical token sequence  
130  $e^{pos} = (s_a^*, s_b^*, s_c^*)$ . Inspired by curriculum learning, we define a scheduling function  $f(t, e^{pos})$   
131 that truncates  $e^{pos}$  and progressively shortens the retained prefix as the training step  $t$  increases.  
132 The resulting truncated prefix is concatenated with the original input to construct a new prompt.  
133 The policy then produces a continuation and the reward is computed accordingly. In this way,  
134 the model starts by predicting lower-level tokens conditioned on higher-level prefixes and  
135 gradually transitions to prefix-free generation, thereby achieving autonomous exploration and  
136 performance gains on difficult samples.

137 (b) **SID-Level Reward Modeling.** We employ GRPO to optimize the LLM with fine-grained, SID-  
138 level rewards. For hard samples whose original rewards are often zero, we treat the step-by-step  
139 generation of the SID path  $\langle a \rangle \rightarrow \langle b \rangle \rightarrow \langle c \rangle$  as an intermediate reasoning process. Suppose  
140 the ground-truth SID token be  $e^{pos} = (s_a^*, s_b^*, s_c^*)$  and the model output be  $e = (s_a, s_b, s_c)$ . A  
141 partial reward is granted according to the deepest level that still matches the ground truth, *i.e.*,  
142  $\kappa(e, e^{pos}) = \max\{k : e_{a:k} = e_{a:k}^*\}$ , preventing zero-reward collapse on hard examples.

143 We evaluate SINGER on two public benchmark datasets (Hou et al., 2024) and compare it with a  
144 wide range of leading traditional sequential recommenders, generative recommenders, and several  
145 recent LLM-based baselines. The results show that SINGER consistently outperforms all competitors  
146 on standard recommendation metrics, confirming its effectiveness. *A detailed survey of related work  
is deferred to Appendix A.*

## 148 2 PRELIMINARY

### 149 2.1 RQ-KMEANS

150 For each item  $i$ , we concatenate its title and textual description and feed the resulting sentence into a  
151 frozen content encoder to produce a  $d$ -dimensional semantic vector  $\mathbf{x} \in \mathbb{R}^d$ . The continuous vector  
152 is then discretized with the RQ-Kmeans algorithm (Luo et al., 2024), which builds a hierarchy of  
153 codebooks by recursively clustering the residuals.

154 Let  $\tilde{\mathbf{M}} = [\mathbf{x}_1; \dots; \mathbf{x}_N] \in \mathbb{R}^{N \times d}$  be the matrix that stacks the embeddings of all  $N$  items. We  
155 initialize  $\mathbf{R}^{(1)} = \tilde{\mathbf{M}}$ . For each layer  $l \in \{1, \dots, L\}$ , where  $L$  is the number of hierarchical levels  
156 in the semantic codebook, we learn a codebook  $\mathbf{C}^{(l)} = \{\mathbf{c}_k^{(l)}\}_{k=1}^{K_l}$  by running K-means with  $K_l$   
157 centroids on the current residuals  $\mathbf{R}^{(l)}$ :

$$158 \mathbf{C}^{(l)} = \text{K-means}(\mathbf{R}^{(l)}, K_l).$$

162 For item  $i$  ( $1 \leq i \leq N$ ), the index of the nearest centroid is obtained via  
 163

$$164 \quad s_i^{(l)} = \arg \min_k \|\mathbf{R}_i^{(l)} - \mathbf{c}_k^{(l)}\|_2, \\ 165$$

166 where  $\|\cdot\|$  denotes the Euclidean norm. The residual is updated as  
 167

$$168 \quad \mathbf{R}_i^{(l+1)} = \mathbf{R}_i^{(l)} - \mathbf{c}_{s_i^{(l)}}^{(l)}. \\ 169$$

170 After  $L = 3$  layers we obtain a coarse-to-fine set of semantic identifiers,  $\{s_i^{(1)}, s_i^{(2)}, s_i^{(3)}\}$ , which  
 171 serves as the unique token sequence for item  $i$  and will be consumed by the recommender for  
 172 progressive generation.  
 173

## 2.2 GROUP-RELATIVE POLICY OPTIMIZATION

175 We fine-tune our policy with the GRPO algorithm (Shao et al., 2024; DeepSeek-AI et al., 2024),  
 176 which leverages the relative quality of multiple responses generated for the same prompt. Concretely,  
 177 for each input  $x \sim D$ , we roll out the current policy  $\pi_{\theta_{\text{old}}}$   $G$  times to obtain a set of candidates  
 178  $\mathcal{Y}(x) = \{y^{(1)}, \dots, y^{(G)}\}$ . Each candidate  $y^{(i)}$  receives a scalar reward  $R_i$ , and the advantage is  
 179 computed by normalizing the rewards *within the group*  
 180

$$181 \quad \hat{A}_i = \frac{R_i - \text{mean}(R_{1:G})}{\text{std}(R_{1:G})}, \quad (1) \\ 182$$

183 where  $R_{1:G} = \{R_1, \dots, R_G\}$ . This groupwise normalization recenters advantages at zero and  
 184 rescales them to unit variance, thereby turning each prompt into a self-contained comparison game  
 185 and reducing gradient variance. The new policy  $\pi_{\theta}$  maximizes the clipped surrogate  
 186

$$187 \quad J_{\text{GRPO}}(\theta) = \mathbb{E}_{x \sim D, y^{(i)} \sim \pi_{\theta_{\text{old}}}} \left[ \frac{1}{G} \sum_{i=1}^G \frac{1}{|y^{(i)}|} \sum_{t=1}^{|y^{(i)}|} \left\{ \min(r_{i,t} \hat{A}_{i,t}, \text{clip}(r_{i,t}, 1 - \epsilon, 1 + \epsilon) \hat{A}_{i,t}) \right. \right. \\ 188 \quad \left. \left. - \beta \text{KL}[\pi_{\theta} \|\pi_{\text{ref}}] \right\} \right], \\ 189 \\ 190 \\ 191 \\ 192 \quad (2)$$

193 where  $r_{i,t} = \frac{\pi_{\theta}(y_t^{(i)} | x, y_{<t}^{(i)})}{\pi_{\theta_{\text{old}}}(y_t^{(i)} | x, y_{<t}^{(i)})}$  is the per-token importance ratio,  $\epsilon$  is the clipping threshold. The term  
 194  $\beta$  balances the task reward against a KL penalty, keeping the updated policy close to the reference  
 195 model  $\pi_{\text{ref}}$ , which is the frozen initial SFT policy.  
 196

## 197 2.3 TASK FORMULATION

198 Generative recommendation reformulates the recommendation problem as a sequence generation  
 199 task. Let  $H_u$  denote the interaction history of user  $u$ , sorted in chronological order. Each item  $i \in H_u$   
 200 is represented by a 3-level SID tuple  $\{s_i^{(1)}, s_i^{(2)}, s_i^{(3)}\}$ . Given  $H_u$ , the generative recommender  $\pi_{\theta}$ ,  
 201 parameterized by  $\theta$ , is trained to predict an item  $i^{\text{pos}}$  that best matches the preferences of user  $u$  from  
 202 the item set. During inference, we employ beam search to generate the top- $k$  candidates and evaluate  
 203 the model with standard generative-recommendation metrics.  
 204

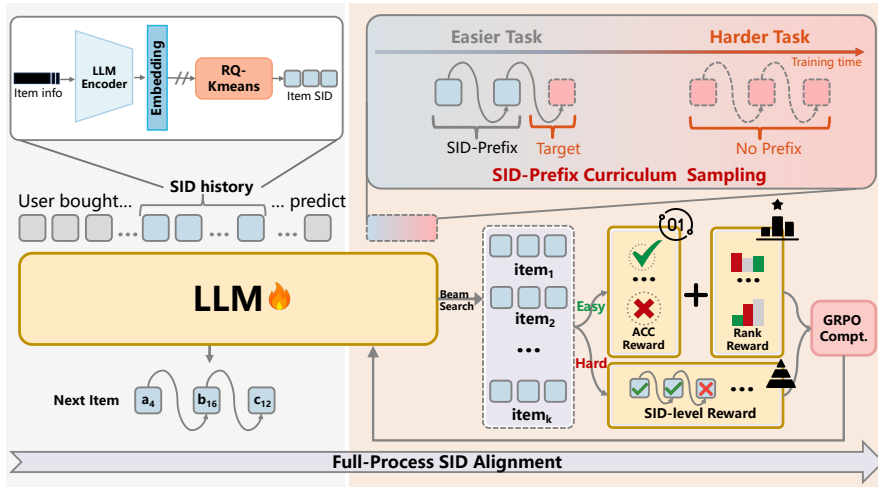
## 205 3 METHODOLOGY

206 To address the key shortcomings of the existing SFT-then-RL pipeline for generative recommendation,  
 207 we propose **SINGER**. The framework elevates the performance ceiling by aligning the LLM with the  
 208 SID space throughout the entire training process and applying SID-navigated optimization in the RL  
 209 stage, as illustrated in Figure 3.  
 210

### 211 3.1 FULL-PROCESS SID ALIGNMENT

212 As demonstrated in Section 1, aligning world knowledge with item SIDs is beneficial for generative  
 213 recommendation (Zheng et al., 2024). Hence, instead of the paradigm that trains only on SIDs  
 214

216  
217  
218  
219  
220  
221  
222  
223  
224  
225  
226  
227  
228  
229  
230  
231



232 Figure 3: SINGER framework. RQ-Kmeans builds the item SID codebook and SFT first aligns  
233 the LLM. In RL, beam search with a SID-prefix curriculum progressively shortens the given prefix,  
234 thereby hardening the task while matching the inference setup. Hit cases receive an accuracy–rank  
235 reward, whereas a SID-level reward grants partial credit to semantically close SIDs when no hit  
236 is found, alleviating sparse feedback. GRPO updates the policy, and SID alignment is enforced  
237 end-to-end.

238 (Rajput et al., 2023; Deng et al., 2025; Wang et al., 2025a), our LLM-based recommender explicitly  
239 strengthens the link between language understanding and collaborative semantics by injecting a set  
240 of alignment objectives:

- 242 • **Semantic Tasks.** Given a chronologically ordered sequence of historical SIDs and an explicit task  
243 instruction, the LLM is asked to predict the SID of the next item the user is likely to interact with.
- 244 • **Alignment Tasks.** It comprises a series of alignment tasks between the textual space and the SID  
245 space. Through these tasks, we encourage a bidirectional mapping that grounds SIDs in language  
246 and injects linguistic knowledge into SID representations.

247 Representative tasks from each category are jointly optimized throughout the entire SFT-then-RL  
248 pipeline, enabling the LLM to fully exploit its world knowledge, deepen its understanding of SIDs,  
249 and ultimately boost generative-recommendation performance. During the RL phase, we employ  
250 constrained decoding, limiting the output space to a precompiled dictionary that contains the SID  
251 of each item as well as its canonical title. This restriction ensures that the LLM can emit only legal  
252 identifiers, making it straightforward to compute a rule-based, verifiable reward signal. Detailed  
253 examples of the prompts are provided in the Appendix D.

### 255 3.2 SID-NATIGATED REINFORCEMENT LEARNING

257 To fully exploit the fine-grained signals carried by SIDs, we introduce SID-Natigated Reinforcement  
258 Learning (SIN-RL). SIN-RL comprises two complementary components—curriculum sampling and  
259 reward modeling. By leveraging the codebook’s inherent coarse-to-fine hierarchy, SIN-RL steers  
260 the agent toward harder examples in a structured manner, thereby improving its capability in the  
261 challenging regions of the data distribution.

#### 262 3.2.1 SID-PREFIX CURRICULUM SAMPLING

264 We first optimize the sampling strategy to preserve rollout diversity in RL for generative recommenda-  
265 tion. In conventional LLM–RL training, LLM first applies dynamic sampling to obtain several  
266 candidate outputs and then computes a group-level reward. Recent studies, however, report a rapid  
267 entropy drop during RL, which harms diversity (Wang et al., 2025b; Cui et al., 2025; He et al.,  
268 2025b; Mukherjee et al., 2025). Inspired by these findings, we use a new sampling strategy tailored  
269 to generative recommendation so as to keep rollouts diverse. Specifically, when  $k$  trajectories are  
required, we do not run  $k$  independent dynamic samplings, each predicting a single item. Instead,

270 we execute one beam-search pass and take the top- $k$  item SIDs as the trajectory set for subsequent  
 271 reward estimation. Following prior work (Bao et al., 2024), we remove length normalization in beam  
 272 search to avoid bias amplification in the LLM-based recommender.

273 Furthermore, we label a training instance  $(x, y^*)$  as difficult when none of the  $k$  items generated  
 274 in the current rollout matches the ground-truth SIDs  $y^*$ . Once normal and hard tasks are separated,  
 275 every hard sample  $(x, y^*) \in \mathcal{D}_{\text{sin}}$  is handled with a SID-Prefix curriculum schedule. At the beginning  
 276 of training, we expose a long SID prefix; as learning progresses, the length of this prefix is gradually  
 277 shortened, encouraging the model to explore on its own. Formally, we use  $p(t)$  to control the length  
 278 of the SID-prefix:

$$279 \quad p(t) = 1 - \frac{t}{T} \quad (3)$$

281 where  $T$  is the total number of RL steps and  $t$  is the current step. Therefore, the value  $p(t)$  decreases  
 282 linearly from 1 to 0, so the depth of the prefix guidance diminishes accordingly throughout training.

283 For every hard instance  $(x, y^*) \in \mathcal{D}_{\text{sin}}$ , we first compute the length of the SID-prefix,  $L_{\text{guide}}$ ,  
 284 according to the schedule  $p(t)$ :

$$285 \quad L_{\text{guide}} = \lfloor p(t) \cdot L \rfloor \quad (4)$$

287 where  $\lfloor \cdot \rfloor$  is the floor operator. We then truncate  $y^*$  to its first  $L_{\text{guide}}$  tokens, denoted by  $y_{L_{\text{guide}}}^*$ , and  
 288 concatenate it with the original input  $x$  to form a new prompt:

$$289 \quad x_{\text{sin}} = x \oplus y_{L_{\text{guide}}}^* \quad (5)$$

291 Finally, the policy produces a continuation  $y \sim \pi_{\theta}(\cdot | x_{\text{sin}})$ , upon which the RL reward is evaluated.

### 293 3.2.2 SID-LEVEL REWARD MODELING

295 For a sampled item  $e_i$  generated by the model, the naive rule-based reward  $R_{\text{acc}}$  follows a binary  
 296 scheme. The ground-truth item  $e^{\text{pos}}$  is assigned 1, whereas every other candidate receives 0, as shown  
 297 below:

$$298 \quad R_{\text{acc}}(e_i) = \begin{cases} 1, & e_i = e^{\text{pos}}, \\ 0, & \text{otherwise.} \end{cases} \quad (6)$$

300 Such sparsity treats all negative samples equally and thus fails to reflect their different levels of  
 301 hardness. We first follow the recent paradigm by constructing an auxiliary ranking score  $R_{\text{rank}}$  that  
 302 exploits the ordering information among candidate items. Specifically, a negative sample that appears  
 303 higher in the generation list (i.e. is produced with a larger probability) should be penalized more. Let  
 304  $p_i$  denote the position of a negative item  $e_i^{\text{neg}}$ . Its ranking reward is defined as the negative reciprocal  
 305 of the natural logarithm of  $(p_i + 1)$ , while the correct item  $e^{\text{pos}}$  is given 0:

$$307 \quad R_{\text{rank}}(e_i) = \begin{cases} 0, & e_i = e^{\text{pos}}, \\ -\frac{1}{\log(p_i + 1)}, & \text{otherwise.} \end{cases} \quad (7)$$

311 Although the ranking reward supplies denser guidance, it still evaluates the whole sequence  $\langle a \rangle \langle b \rangle \langle c \rangle$   
 312 as a single target and overlooks the multi-granular clues embedded in the SID codebook. Conse-  
 313 quently, for many difficult instances  $(x, y^*) \in \mathcal{D}_{\text{sin}}$  the reward may still collapse to zero, leaving the  
 314 sparsity issue unsolved.

315 To address this limitation, we further view the generation of the hierarchical SID  $\langle a \rangle \rightarrow \langle b \rangle \rightarrow \langle c \rangle$   
 316 as a step-by-step inference process and design SID-level reward. Instead of relying on external  
 317 Process-Reward Models, the proposed approach harnesses the codebook’s innate coarse-to-fine  
 318 hierarchy to provide intermediate reasoning signals at each SID layer. This objective can be formally  
 319 expressed as:

$$320 \quad R_{\text{reason}}(e_i) = 1 - \lambda^k \quad (8)$$

321 where  $k = f(e_i, e^{\text{pos}})$  denotes the deepest layer at which the generated sequence  $e_i$  matches  
 322 the ground-truth sequence  $e^{\text{pos}}$ , and  $\lambda \in (0, 1)$  is a decay coefficient that modulates the reward  
 323 increment across different layers and guarantees that the overall reward always lies in the interval  
 $0 < R_{\text{reason}}(e_i) < 1$ . The final total reward can be formally expressed as:

---

324  
 325  

$$R(e_i) = \begin{cases} R_{\text{acc}}(e^i) + R_{\text{rank}}(e^i), & (x, y^*) \notin \mathcal{D}_{\text{sin}}, \\ R_{\text{reason}}(e^i), & \text{otherwise.} \end{cases} \quad (9)$$
  
 326  
 327  
 328

329 For challenging samples  $(x, y^*) \in \mathcal{D}_{\text{sin}}$ , SID-Level Reward Modeling fully exploits SID’s hierarchi-  
 330 cal rewards to deliver fine-grained guidance.

331  
 332 **4 EXPERIMENTS**  
 333

334 In this section, we first report the empirical performance of **SINGER** on two real-world benchmarks  
 335 (Hou et al., 2024), and compare it against a selected set of baselines covering conventional sequential  
 336 recommenders, SID-based generative models, and recent LLM-powered recommenders. In addition,  
 337 we recast the SID-based next-item prediction task as recommendation rule discovery and show that  
 338 **SINGER** offers extra gains for cold-start users with scarce interactions and even for completely  
 339 unseen domains. We further conduct extensive ablation studies to pinpoint the components that most  
 340 contribute to **SINGER**’s effectiveness. Refer to the appendix B for detailed implementation details.  
 341 In short, this section is organized to answer the following research questions:

342 • **RQ1:** How does **SINGER** perform in comparison to other baseline methods?  
 343 • **RQ2:** How does **SINGER** perform under completely unseen domains?  
 344 • **RQ3:** How do the designed components contribute to **SINGER**’s recommendation efficacy?

345 **Datasets and Metrics.** We conduct extensive experiments on two real-world subsets of the Amazon  
 346 Review corpus—*Office* and *Industrial*. Following common practice, we adopt Hit Rate (HR@K)  
 347 and Normalized Discounted Cumulative Gain (NDCG@K) to evaluate the top- $K$  recommendation  
 348 accuracy. Please refer to Appendix B for more details about datasets and evaluation metrics.

349 **Baselines.** Our baselines contain three categories: (1) Traditional recommendation models, including  
 350 GRU4Rec (Hidasi et al., 2016), Caser (Tang and Wang, 2018), SASRec (Kang and McAuley, 2018);  
 351 (2) Generative recommendation models: HSTU (Zhai et al., 2024), TIGER (Rajput et al., 2023),  
 352 LC-Rec (Zheng et al., 2024); (3) LLM-based recommendation models, including BigRec (Bao et al.,  
 353 2023), D3 (Bao et al., 2024), S-DPO (Chen et al., 2024). Please see Appendix B for more information.

354  
 355 **4.1 PERFORMANCE COMPARISON (RQ1)**  
 356

357 We conduct a comprehensive evaluation of **SINGER** on three benchmark datasets—*Industrial* and  
 358 *Toys*; the results are summarized in Table 1. Two major observations emerge:

359 • **Utility of LLM World Knowledge.** LLM-based recommenders such as BIGRec and D<sup>3</sup> markedly  
 360 outperform classical paradigms like GRU4Rec and Caser, confirming that injecting the broad world  
 361 knowledge encoded in LLMs can substantially boost recommendation quality.  
 362 • **Effectiveness of SINGER.** By incorporating fine-grained SID information into the RL loop and  
 363 aligning the entire generation trajectory with the task objective, **SINGER** establishes new SOTA  
 364 across all three datasets, significantly surpassing the strongest prior baselines.

365  
 366 **4.2 UNSEEN-DOMAIN PERFORMANCE EVALUATION (RQ2)**  
 367

368 To assess **SINGER**’s generalization to out-of-distribution (OOD) data, we conduct an unseen-domain  
 369 study termed *SID pattern discovery*. Specifically, the model is trained on the source domain *Industrial*  
 370 and evaluated on a completely unseen target domain *Office*. Given that prior studies have shown  
 371 SFT can overfit to the training domain and degrade OOD performance (Jin et al., 2025; Yue et al.,  
 372 2025; Yoshihara et al., 2025; Cheng et al., 2025), we introduce an RL-only variant, **SINGER-w/ RL**,  
 373 specifically to provide a version focused on OOD generalization. We benchmark three systems: (1)  
 374 GRU4Rec, trained and tested on *Office*. (2) Qwen-Text, which encodes the user’s interaction history  
 375 as plain text and predicts the next item in textual form; (3) Qwen-SID, which represents the same  
 376 history as a sequence of SIDs and predicts the next SID; (4) **SINGER-w/ RL**, which is trained solely  
 377 with RL on *Industrial* and is tested on *Office* without SFT.

378 Table 1: Performance of SINGER Compared to Traditional Methods, Generative Methods, and  
 379 LLM-based Methods

Dateset	Methods	HR@3	NDCG@3	HR@5	NDCG@5	HR@10	NDCG@10
<b>Traditional</b>							
	GRU4Rec	0.0638	0.0542	0.0774	0.0598	0.0999	0.0669
	Caser	0.0618	0.0514	0.0717	0.0555	0.0942	0.0628
	SASRec	0.0790	0.0700	0.0909	0.0748	0.1088	0.0806
<b>Generative</b>							
<b>Industrial</b>	HSTU	0.0927	0.0885	0.1037	0.0918	0.1163	0.0958
	TIGER	0.0852	0.0742	0.1010	0.0807	0.1321	0.0908
	LCRec	0.0915	0.0805	0.1057	0.0862	0.1332	0.0952
	<b>LLM-based</b>						
	BIGRec	0.0931	0.0841	0.1092	0.0907	0.1370	0.0997
	D <sup>3</sup>	0.1024	<u>0.0991</u>	0.1213	0.0989	0.1500	<u>0.1082</u>
	S-DPO	0.1032	0.0906	<u>0.1238</u>	<u>0.0991</u>	<u>0.1524</u>	<u>0.1082</u>
<b>Ours</b>							
	<b>SINGER</b>	<b>0.1256</b>	<b>0.1112</b>	<b>0.1453</b>	<b>0.1192</b>	<b>0.1744</b>	<b>0.1276</b>
<b>Traditional</b>							
<b>Office</b>	GRU4Rec	0.0629	0.0528	0.0789	0.0595	0.1019	0.0669
	Caser	0.0748	0.0615	0.0865	0.0664	0.1093	0.0737
	SASRec	0.0861	0.0769	0.0949	0.0805	0.1120	0.0858
	<b>Generative</b>						
	HSTU	0.1134	0.1031	0.1252	0.1079	0.1400	0.1126
	TIGER	0.0986	0.0852	0.1163	0.0960	0.1408	0.1002
	LCRec	0.0921	0.0807	0.1048	0.0859	0.1237	0.0920
<b>LLM-based</b>							
	BIGRec	0.1069	0.0961	0.1204	0.1017	0.1434	0.1091
	D <sup>3</sup>	<u>0.1204</u>	<u>0.1055</u>	<u>0.1406</u>	<u>0.1139</u>	<u>0.1634</u>	0.1213
	S-DPO	0.1169	0.1033	0.1356	0.1110	0.1587	<u>0.1255</u>
<b>Ours</b>							
	<b>SINGER</b>	<b>0.1331</b>	<b>0.1163</b>	<b>0.1472</b>	<b>0.1221</b>	<b>0.1746</b>	<b>0.1309</b>

407 Table 2: Performance of SINGER and its variants on completely unseen recommendation domains

Dataset	Method	HR@3	NDCG@3	HR@5	NDCG@5	HR@10	NDCG@10
<b>Office</b>	GRU4Rec	0.0629	0.0528	0.0789	0.0595	0.1019	0.0669
	Qwen-Text	0.0031	0.0021	0.0044	0.0026	0.0057	0.0030
	Qwen-SID	0.0300	0.0214	0.0456	0.0282	0.0733	0.0373
	SINGER-w/ RL	0.0553	<u>0.0433</u>	<u>0.0691</u>	<u>0.0489</u>	<u>0.0892</u>	<u>0.0553</u>

416 As reported in Table 2, Qwen-Text performs rather poorly, whereas Qwen-SID is markedly better,  
 417 demonstrating that the structured SID space is easier for a language model to exploit. Although  
 418 SINGER-w/ RL lags behind the full SINGER on in-domain metrics, its RL-only optimization offers  
 419 strong transferability, yielding competitive accuracy on the unseen Office catalogue surprisingly.  
 420 Despite the substantial domain shift and the possible semantic mismatch among SIDs, SINGER  
 421 can still discover transferable interaction patterns and produce high-quality recommendations for a  
 422 brand-new catalogue, highlighting the encouraging unseen-domain potential of our framework.

### 4.3 ABLATION STUDY (RQ3)

425 To validate the effectiveness of each component in the SINGER framework, we compare it with the  
 426 following alternative approaches.

#### 4.3.1 ALIGNING STRATEGY

430 We benchmark the full model against three carefully designed variants: (1) SINGER-w/o ALIGN: A  
 431 pure SID→SID paradigm: the input consists of SID-organized user histories, and the target is the SID  
 of the next item. No cross-modal alignment is applied in either stage. (2) SINGER-w/ SFTALIGN:

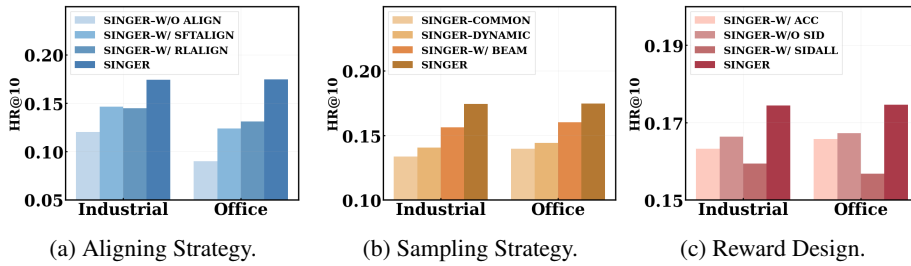


Figure 4: Study on the effectiveness of SINGER’s individual components. Figure 4a examines model performance under different alignment strategies; Figure 4b investigates various sampling strategies; Figure 4c evaluates the impact of alternative reward designs.

Alignment tasks are used only during the SFT stage, whereas the RL stage is trained on SID-only data. (3) SINGER-w/ RLALIGN: The SFT stage relies on SID-only supervision, while alignment tasks are introduced solely in the RL stage.

As illustrated in Figure 4a, the full SINGER with full-process SID alignment achieves the best results across all metrics. The SINGER-w/o ALIGN variant performs the worst, underscoring the importance of grounding world knowledge when generating SIDs. Notably, although introducing the alignment objective directly in the RL stage is highly challenging for an LLM that has not been pre-conditioned by SFT, SINGER-w/ RLALIGN still yields a non-trivial gain. We attribute this improvement to our SID-Guided RL scheme, which offers the agent additional opportunities to obtain valid rewards on hard examples that conventional RL would likely miss.

#### 4.3.2 SAMPLING STRATEGY

We contrast the full model with three variants that differ only in the way trajectories are collected: (1) SINGER–COMMON that uses a conventional top- $k$  decoding scheme to generate the required number of trajectories. (2) SINGER–DYNAMIC, which implements our dynamic sampler that first produces  $\frac{3}{2}$  times the target trajectory budget and then keeps as many distinct items as possible for RL optimization. (3) SINGER–w/ BEAM that retains only beam search; no SID-prefix guidance is applied, and all examples maintain their original difficulty level.

As Figure 4b illustrates, the full SINGER achieves the best overall performance. Moreover, the SINGER-w/ BEAM variant attains higher accuracy than SINGER–DYNAMIC while requiring only two-thirds of its sampling budget, showing that beam search is a more cost-effective backbone. These findings motivate our final design that merges beam search with SID-prefix guidance.

#### 4.3.3 REWARD DESIGN

Three variants are compared: (1) SINGER-w/ ACC that uses the accuracy reward only; (2) SINGER-w/o SID that removes the SID-level reward for hard cases; the LLM is optimized with the accuracy plus rank rewards. (3) SINGER-w/ SIDALL that applies the SID-level reward to every training sample rather than restricting it to difficult ones.

As shown in the Figure 4c, the full model, which deploys SID-level reward only for hard samples, achieves the best overall performance. To be noticed, rewarding all samples at the SID-level slightly degrades performance. We hypothesize that, for easy instances already covered by the accuracy and ranking rewards, an additional SID-level signal may dilute the optimization focus and introduce a mismatch with the evaluation metrics (HR@K and NDCG@K). For hard cases, however, the hierarchical structure encoded in SIDs provides intermediate guidance where conventional rewards are sparse, steering the model toward correct reasoning paths.

## 5 CONCLUSION

This paper investigates how the *SFT-then-RL* paradigm, which has recently proved successful in language–reasoning tasks, can be adapted to the generative recommendation setting. Through a careful analysis, we identify two central obstacles — limited SID understanding and ineffective

---

486 reward assignment — that prevent a direct transfer of the vanilla pipeline. To overcome these issues,  
487 we propose **SINGER**, a SID-Navigated GEnenerative Recommender that (i) performs Full-Process  
488 SID Alignment to inject SID-aware objectives into every stage of post-training, and (ii) introduces  
489 SID-Navigated RL, which supplies fine-grained SID-level rewards and a hierarchy-based curriculum  
490 sampler. Experiments on two public benchmarks demonstrate consistent improvements over SOTA  
491 sequential, generative, and LLM-based recommenders, showing that deep SID comprehension and  
492 SID-Navigated RL feedback are both indispensable for unleashing the full potential of LLMs in  
493 recommendation.

494

495

496

497

498

499

500

501

502

503

504

505

506

507

508

509

510

511

512

513

514

515

516

517

518

519

520

521

522

523

524

525

526

527

528

529

530

531

532

533

534

535

536

537

538

539

---

540 CLAIM

541

542 5.1 ETHICS STATEMENT

543

544 Our study relies exclusively on publicly available benchmark datasets that contain no personally-  
545 identifiable information. Data collection, storage, and processing strictly follow the licences and  
546 terms of use provided by the original publishers. All LLMs employed in this work are open-sourced  
547 and used under their respective permissive licences. We make no attempt to infer sensitive attributes  
548 of users, and all generated recommendations are produced within a controlled, offline research  
549 environment. The authors declare that no conflict of interest exists.

550

551 5.2 REPRODUCIBILITY STATEMENT

552

553 We take reproducibility seriously and adopt the following measures: 1) All source code, configuration  
554 files, and experiment scripts will be released upon publication. 2) We provide detailed instructions  
555 for environment setup, including package versions, CUDA/driver requirements. 3) Random seeds  
556 are fixed for data splitting, parameter initialization, and sampling operations. 4) Pre-processed  
557 datasets, together with the raw-to-processed conversion scripts, are included to guarantee identical  
558 data partitions.

559

560

561

562

563

564

565

566

567

568

569

570

571

572

573

574

575

576

577

578

579

580

581

582

583

584

585

586

587

588

589

590

591

592

593

---

## 594 REFERENCES

## 595

596 Keqin Bao, Jizhi Zhang, Wenjie Wang, Yang Zhang, Zhengyi Yang, Yancheng Luo, Fuli Feng, Xiang-  
597 nan He, and Qi Tian. A bi-step grounding paradigm for large language models in recommendation  
598 systems. *CoRR*, abs/2308.08434, 2023.

599 Leheng Sheng, An Zhang, Yi Zhang, Yuxin Chen, Xiang Wang, and Tat-Seng Chua. Language  
600 models encode collaborative signals in recommendation. *arXiv preprint arXiv:2407.05441*, 2024.

601 Guoqing Hu, An Zhang, Shuo Liu, Zhibo Cai, Xun Yang, and Xiang Wang. Alphafuse: Learn ID  
602 embeddings for sequential recommendation in null space of language embeddings. In *SIGIR*, 2025.

603

604 Yingzhi He, Xiaohao Liu, An Zhang, Yunshan Ma, and Tat-Seng Chua. Llm2rec: Large language  
605 models are powerful embedding models for sequential recommendation. In *KDD*, 2025a.

606 Likang Wu, Zhi Zheng, Zhaopeng Qiu, Hao Wang, Hongchao Gu, Tingjia Shen, Chuan Qin, Chen  
607 Zhu, Hengshu Zhu, Qi Liu, Hui Xiong, and Enhong Chen. A survey on large language models for  
608 recommendation. *World Wide Web (WWW)*, 2024.

609

610 Hui Fang, Danning Zhang, Yiheng Shu, and Guibing Guo. Deep learning for sequential recommen-  
611 dation: Algorithms, influential factors, and evaluations. *ACM Trans. Inf. Syst.*, 2020.

612 Shashank Rajput, Nikhil Mehta, Anima Singh, Raghunandan Hulikal Keshavan, Trung Vu, Lukasz  
613 Heldt, Lichan Hong, Yi Tay, Vinh Q. Tran, Jonah Samost, Maciej Kula, Ed H. Chi, and Mahesh  
614 Sathiamoorthy. Recommender systems with generative retrieval. In *Advances in Neural Information  
615 Processing Systems 36: Annual Conference on Neural Information Processing Systems 2023,  
616 NeurIPS 2023, New Orleans, LA, USA, December 10 - 16, 2023*, 2023.

617 Bowen Zheng, Yupeng Hou, Hongyu Lu, Yu Chen, Wayne Xin Zhao, Ming Chen, and Ji-Rong Wen.  
618 Adapting large language models by integrating collaborative semantics for recommendation. In  
619 *40th IEEE International Conference on Data Engineering, ICDE 2024, Utrecht, The Netherlands,  
620 May 13-16, 2024*. IEEE, 2024.

621 Haohao Qu, Wenqi Fan, Zihuai Zhao, and Qing Li. Tokenrec: Learning to tokenize ID for llm-based  
622 generative recommendation. *CoRR*, abs/2406.10450, 2024.

623

624 Jiaqi Zhai, Lucy Liao, Xing Liu, Yueming Wang, Rui Li, Xuan Cao, Leon Gao, Zhaojie Gong, Fangda  
625 Gu, Jiayuan He, Yinghai Lu, and Yu Shi. Actions speak louder than words: Trillion-parameter  
626 sequential transducers for generative recommendations. In *Forty-first International Conference on  
627 Machine Learning, ICML 2024, Vienna, Austria, July 21-27, 2024*. OpenReview.net, 2024. URL  
628 <https://openreview.net/forum?id=xye7iNsgXn>.

629 Jiaxin Deng, Shiyao Wang, Kuo Cai, Lejian Ren, Qigen Hu, Weifeng Ding, Qiang Luo, and Guorui  
630 Zhou. Onerec: Unifying retrieve and rank with generative recommender and iterative preference  
631 alignment. *CoRR*, abs/2502.18965, 2025.

632 Yuxiang Wang, Xiao Yan, Chi Ma, Mincong Huang, Xiaoguang Li, Lei Yu, Chuan Liu, Ruidong Han,  
633 He Jiang, Bin Yin, Shangyu Chen, Fei Jiang, Xiang Li, Wei Lin, Haowei Han, Bo Du, and Jiawei  
634 Jiang. Mtgrboost: Boosting large-scale generative recommendation models in meituan. *CoRR*,  
635 abs/2505.12663, 2025a.

636 Neil Zeghidour, Alejandro Luebs, Ahmed Omran, Jan Skoglund, and Marco Tagliasacchi. Sound-  
637 stream: An end-to-end neural audio codec. *IEEE ACM Trans. Audio Speech Lang. Process.*, 30,  
638 2022.

639

640 Xincheng Luo, Jiangxia Cao, Tianyu Sun, Jinkai Yu, Rui Huang, Wei Yuan, Hezheng Lin, Yichen  
641 Zheng, Shiyao Wang, Qigen Hu, Changqing Qiu, Jiaqi Zhang, Xu Zhang, Zhiheng Yan, Jingming  
642 Zhang, Simin Zhang, Mingxing Wen, Zhaojie Liu, Kun Gai, and Guorui Zhou. QARM: quantitative  
643 alignment multi-modal recommendation at kuaishou. *CoRR*, abs/2411.11739, 2024.

644 Anima Singh, Trung Vu, Nikhil Mehta, Raghunandan H. Keshavan, Maheswaran Sathiamoorthy,  
645 Yilin Zheng, Lichan Hong, Lukasz Heldt, Li Wei, Devansh Tandon, Ed H. Chi, and Xinyang  
646 Yi. Better generalization with semantic ids: A case study in ranking for recommendations. In  
647 *Proceedings of the 18th ACM Conference on Recommender Systems, RecSys 2024, Bari, Italy,  
October 14-18, 2024*. ACM, 2024.

---

648 Ashish Vaswani, Noam Shazeer, Niki Parmar, Jakob Uszkoreit, Llion Jones, Aidan N. Gomez, Lukasz  
649 Kaiser, and Illia Polosukhin. Attention is all you need. In *NIPS*, 2017.  
650

651 Yuxin Chen, Junfei Tan, An Zhang, Zhengyi Yang, Leheng Sheng, Enzhi Zhang, Xiang Wang, and  
652 Tat-Seng Chua. On softmax direct preference optimization for recommendation. In *NeurIPS*, 2024.  
653

654 Zhihong Shao, Peiyi Wang, Qihao Zhu, Runxin Xu, Junxiao Song, Mingchuan Zhang, Y. K. Li,  
655 Y. Wu, and Daya Guo. Deepseekmath: Pushing the limits of mathematical reasoning in open  
656 language models. *CoRR*, 2024.  
657

658 Hiroshi Yoshihara, Taiki Yamaguchi, and Yuichi Inoue. A practical two-stage recipe for mathemat-  
659 ical ILMs: Maximizing accuracy with SFT and efficiency with reinforcement learning. *CoRR*,  
660 abs/2507.08267, 2025.  
661

662 OpenAI, :, Aaron Jaech, Adam Kalai, Adam Lerer, Adam Richardson, Ahmed El-Kishky, Aiden  
663 Low, Alec Helyar, Aleksander Madry, Alex Beutel, Alex Carney, Alex Iftimie, Alex Karpenko,  
664 Alex Tachard Passos, Alexander Neitz, Alexander Prokofiev, Alexander Wei, Allison Tam, Ally  
665 Bennett, Ananya Kumar, Andre Saraiva, Andrea Vallone, Andrew Duberstein, Andrew Kondrich,  
666 Andrey Mishchenko, Andy Applebaum, Angela Jiang, Ashvin Nair, Barret Zoph, Behrooz Ghor-  
667 bani, Ben Rossen, Benjamin Sokolowsky, Boaz Barak, Bob McGrew, Borys Minaiev, Botao  
668 Hao, Bowen Baker, Brandon Houghton, Brandon McKinzie, Brydon Eastman, Camillo Lugaressi,  
669 Cary Bassin, Cary Hudson, Chak Ming Li, Charles de Bourcy, Chelsea Voss, Chen Shen, Chong  
670 Zhang, Chris Koch, Chris Orsinger, Christopher Hesse, Claudia Fischer, Clive Chan, Dan Roberts,  
671 Daniel Kappler, Daniel Levy, Daniel Selsam, David Dohan, David Farhi, David Mely, David  
672 Robinson, Dimitris Tsipras, Doug Li, Dragos Oprica, Eben Freeman, Eddie Zhang, Edmund Wong,  
673 Elizabeth Proehl, Enoch Cheung, Eric Mitchell, Eric Wallace, Erik Ritter, Evan Mays, Fan Wang,  
674 Felipe Petroski Such, Filippo Raso, Florencia Leoni, Foivos Tsimpourlas, Francis Song, Fred  
675 von Lohmann, Freddie Sulit, Geoff Salmon, Giambattista Parascandolo, Gildas Chabot, Grace  
676 Zhao, Greg Brockman, Guillaume Leclerc, Hadi Salman, Haiming Bao, Hao Sheng, Hart Andrin,  
677 Hessam Bagherinezhad, Hongyu Ren, Hunter Lightman, Hyung Won Chung, Ian Kivlichan, Ian  
678 O'Connell, Ian Osband, Ignasi Clavera Gilaberte, Ilge Akkaya, Ilya Kostrikov, Ilya Sutskever,  
679 Irina Kofman, Jakub Pachocki, James Lennon, Jason Wei, Jean Harb, Jerry Twore, Jiacheng Feng,  
680 Jiahui Yu, Jiayi Weng, Jie Tang, Jieqi Yu, Joaquin Quiñonero Candela, Joe Palermo, Joel Parish,  
681 Johannes Heidecke, John Hallman, John Rizzo, Jonathan Gordon, Jonathan Uesato, Jonathan  
682 Ward, Joost Huizinga, Julie Wang, Kai Chen, Kai Xiao, Karan Singhal, Karina Nguyen, Karl  
683 Cobbe, Katy Shi, Kayla Wood, Kendra Rimbach, Keren Gu-Lemberg, Kevin Liu, Kevin Lu, Kevin  
684 Stone, Kevin Yu, Lama Ahmad, Lauren Yang, Leo Liu, Leon Maksin, Leyton Ho, Liam Fedus,  
685 Lilian Weng, Linden Li, Lindsay McCallum, Lindsey Held, Lorenz Kuhn, Lukas Kondraciuk,  
686 Lukasz Kaiser, Luke Metz, Madelaine Boyd, Maja Trebacz, Manas Joglekar, Mark Chen, Marko  
687 Tintor, Mason Meyer, Matt Jones, Matt Kaufer, Max Schwarzer, Meghan Shah, Mehmet Yatbaz,  
688 Melody Y. Guan, Mengyuan Xu, Mengyuan Yan, Mia Glaese, Mianna Chen, Michael Lampe,  
689 Michael Malek, Michele Wang, Michelle Fradin, Mike McClay, Mikhail Pavlov, Miles Wang,  
690 Mingxuan Wang, Mira Murati, Mo Bavarian, Mostafa Rohaninejad, Nat McAleese, Neil Chowd-  
691 hury, Neil Chowdhury, Nick Ryder, Nikolas Tezak, Noam Brown, Ofir Nachum, Oleg Boiko, Oleg  
692 Murk, Olivia Watkins, Patrick Chao, Paul Ashbourne, Pavel Izmailov, Peter Zhokhov, Rachel Dias,  
693 Rahul Arora, Randall Lin, Rapha Gontijo Lopes, Raz Gaon, Reah Miyara, Reimar Leike, Renny  
694 Hwang, Rhythm Garg, Robin Brown, Roshan James, Rui Shu, Ryan Cheu, Ryan Greene, Saachi  
695 Jain, Sam Altman, Sam Toizer, Sam Toyer, Samuel Miserendino, Sandhini Agarwal, Santiago  
696 Hernandez, Sasha Baker, Scott McKinney, Scottie Yan, Shengjia Zhao, Shengli Hu, Shibani  
697 Santurkar, Shraman Ray Chaudhuri, Shuyuan Zhang, Siyuan Fu, Spencer Papay, Steph Lin, Suchir  
698 Balaji, Suvansh Sanjeev, Szymon Sidor, Tal Broda, Aidan Clark, Tao Wang, Taylor Gordon, Ted  
699 Sanders, Tejal Patwardhan, Thibault Sottiaux, Thomas Degry, Thomas Dimson, Tianhao Zheng,  
700 Timur Garipov, Tom Stasi, Trapit Bansal, Trevor Creech, Troy Peterson, Tyna Eloundou, Valerie  
701 Qi, Vineet Kosaraju, Vinnie Monaco, Vitchyr Pong, Vlad Fomenko, Weiyi Zheng, Wenda Zhou,  
DeepSeek-AI, Daya Guo, Dejian Yang, Haowei Zhang, Junxiao Song, Ruoyu Zhang, Runxin Xu,  
Qihao Zhu, Shirong Ma, Peiyi Wang, Xiao Bi, Xiaokang Zhang, Xingkai Yu, Yu Wu, Z. F. Wu,

702 Zhibin Gou, Zhihong Shao, Zhuoshu Li, Ziyi Gao, Aixin Liu, Bing Xue, Bingxuan Wang, Bochao  
703 Wu, Bei Feng, Chengda Lu, Chenggang Zhao, Chengqi Deng, Chenyu Zhang, Chong Ruan,  
704 Damai Dai, Deli Chen, Dongjie Ji, Erhang Li, Fangyun Lin, Fucong Dai, Fuli Luo, Guangbo Hao,  
705 Guanting Chen, Guowei Li, H. Zhang, Han Bao, Hanwei Xu, Haocheng Wang, Honghui Ding,  
706 Huajian Xin, Huazuo Gao, Hui Qu, Hui Li, Jianzhong Guo, Jiaoshi Li, Jiawei Wang, Jingchang  
707 Chen, Jingyang Yuan, Junjie Qiu, Junlong Li, J. L. Cai, Jiaqi Ni, Jian Liang, Jin Chen, Kai Dong,  
708 Kai Hu, Kaige Gao, Kang Guan, Kexin Huang, Kuai Yu, Lean Wang, Lecong Zhang, Liang Zhao,  
709 Litong Wang, Liyue Zhang, Lei Xu, Leyi Xia, Mingchuan Zhang, Minghua Zhang, Minghui Tang,  
710 Meng Li, Miaojun Wang, Mingming Li, Ning Tian, Panpan Huang, Peng Zhang, Qiancheng Wang,  
711 Qinyu Chen, Qiushi Du, Ruiqi Ge, Ruisong Zhang, Ruizhe Pan, Runji Wang, R. J. Chen, R. L.  
712 Jin, Ruyi Chen, Shanghao Lu, Shangyan Zhou, Shanhua Chen, Shengfeng Ye, Shiyu Wang,  
713 Shuiping Yu, Shunfeng Zhou, Shuting Pan, and S. S. Li. Deepseek-r1: Incentivizing reasoning  
714 capability in llms via reinforcement learning. *CoRR*, 2025.

715 Qiying Yu, Zheng Zhang, Ruofei Zhu, Yufeng Yuan, Xiaochen Zuo, Yu Yue, Tiantian Fan, Gaohong  
716 Liu, Lingjun Liu, Xin Liu, Haibin Lin, Zhiqi Lin, Bole Ma, Guangming Sheng, Yuxuan Tong, Chi  
717 Zhang, Mofan Zhang, Wang Zhang, Hang Zhu, Jinhua Zhu, Jiaze Chen, Jiangjie Chen, Chengyi  
718 Wang, Hongli Yu, Weinan Dai, Yuxuan Song, Xiangpeng Wei, Hao Zhou, Jingjing Liu, Wei-Ying  
719 Ma, Ya-Qin Zhang, Lin Yan, Mu Qiao, Yonghui Wu, and Mingxuan Wang. DAPO: an open-source  
720 LLM reinforcement learning system at scale. *CoRR*, abs/2503.14476, 2025.

721 Tianzhe Chu, Yuexiang Zhai, Jihan Yang, Shengbang Tong, Saining Xie, Dale Schuurmans, Quoc V.  
722 Le, Sergey Levine, and Yi Ma. SFT memorizes, RL generalizes: A comparative study of foundation  
723 model post-training. *CoRR*, 2025.

724 Yang Yue, Zhiqi Chen, Rui Lu, Andrew Zhao, Zhaokai Wang, Yang Yue, Shiji Song, and Gao Huang.  
725 Does reinforcement learning really incentivize reasoning capacity in llms beyond the base model?  
726 *CoRR*, abs/2504.13837, 2025.

727 Zichen Liu, Changyu Chen, Wenjun Li, Penghui Qi, Tianyu Pang, Chao Du, Wee Sun Lee, and Min  
728 Lin. Understanding r1-zero-like training: A critical perspective. *CoRR*, abs/2503.20783, 2025.

729 Yupeng Hou, Jiacheng Li, Zhankui He, An Yan, Xiusi Chen, and Julian J. McAuley. Bridging  
730 language and items for retrieval and recommendation. *CoRR*, 2024.

731 DeepSeek-AI, Aixin Liu, Bei Feng, Bing Xue, Bingxuan Wang, Bochao Wu, Chengda Lu, Chenggang  
732 Zhao, Chengqi Deng, Chenyu Zhang, Chong Ruan, Damai Dai, Daya Guo, Dejian Yang, Deli  
733 Chen, Dongjie Ji, Erhang Li, Fangyun Lin, Fucong Dai, Fuli Luo, Guangbo Hao, Guanting Chen,  
734 Guowei Li, H. Zhang, Han Bao, Hanwei Xu, Haocheng Wang, Haowei Zhang, Honghui Ding,  
735 Huajian Xin, Huazuo Gao, Hui Li, Hui Qu, J. L. Cai, Jian Liang, Jianzhong Guo, Jiaqi Ni, Jiaoshi  
736 Li, Jiawei Wang, Jin Chen, Jingchang Chen, Jingyang Yuan, Junjie Qiu, Junlong Li, Junxiao Song,  
737 Kai Dong, Kai Hu, Kaige Gao, Kang Guan, Kexin Huang, Kuai Yu, Lean Wang, Lecong Zhang,  
738 Lei Xu, Leyi Xia, Liang Zhao, Litong Wang, Liyue Zhang, Meng Li, Miaojun Wang, Mingchuan  
739 Zhang, Minghua Zhang, Minghui Tang, Mingming Li, Ning Tian, Panpan Huang, Peiyi Wang,  
740 Peng Zhang, Qiancheng Wang, Qihao Zhu, Qinyu Chen, Qiushi Du, R. J. Chen, R. L. Jin, Ruiqi  
741 Ge, Ruisong Zhang, Ruizhe Pan, Runji Wang, Runxin Xu, Ruoyu Zhang, Ruyi Chen, S. S. Li,  
742 Shanghao Lu, Shangyan Zhou, Shanhua Chen, Shaoqing Wu, Shengfeng Ye, Shengfeng Ye,  
743 Shirong Ma, Shiyu Wang, Shuang Zhou, Shuiping Yu, Shunfeng Zhou, Shuting Pan, T. Wang, Tao  
744 Yun, Tian Pei, Tianyu Sun, W. L. Xiao, and Wangding Zeng. Deepseek-v3 technical report. *CoRR*,  
745 2024.

746 Shenzhi Wang, Le Yu, Chang Gao, Chujie Zheng, Shixuan Liu, Rui Lu, Kai Dang, Xionghui Chen,  
747 Jianxin Yang, Zhenru Zhang, Yuqiong Liu, An Yang, Andrew Zhao, Yang Yue, Shiji Song, Bowen  
748 Yu, Gao Huang, and Junyang Lin. Beyond the 80/20 rule: High-entropy minority tokens drive  
749 effective reinforcement learning for LLM reasoning. *CoRR*, abs/2506.01939, 2025b.

750 Ganqu Cui, Yuchen Zhang, Jiacheng Chen, Lifan Yuan, Zhi Wang, Yuxin Zuo, Haozhan Li, Yuchen  
751 Fan, Huayu Chen, Weize Chen, Zhiyuan Liu, Hao Peng, Lei Bai, Wanli Ouyang, Yu Cheng, Bowen  
752 Zhou, and Ning Ding. The entropy mechanism of reinforcement learning for reasoning language  
753 models. *CoRR*, abs/2505.22617, 2025.

756 Jujie He, Jiacai Liu, Chris Yuhao Liu, Rui Yan, Chaojie Wang, Peng Cheng, Xiaoyu Zhang, Fuxiang  
757 Zhang, Jiacheng Xu, Wei Shen, Siyuan Li, Liang Zeng, Tianwen Wei, Cheng Cheng, Bo An, Yang  
758 Liu, and Yahui Zhou. Skywork open reasoner 1 technical report. *CoRR*, abs/2505.22312, 2025b.  
759

760 Sagnik Mukherjee, Lifan Yuan, Dilek Hakkani-Tur, and Hao Peng. Reinforcement learning finetunes  
761 small subnetworks in large language models. *CoRR*, abs/2505.11711, 2025. doi: 10.48550/ARXIV.  
762 2505.11711. URL <https://doi.org/10.48550/arXiv.2505.11711>.

763 Keqin Bao, Jizhi Zhang, Yang Zhang, Xinyue Huo, Chong Chen, and Fuli Feng. Decoding matters:  
764 Addressing amplification bias and homogeneity issue in recommendations for large language  
765 models. In *Proceedings of the 2024 Conference on Empirical Methods in Natural Language  
766 Processing, EMNLP 2024, Miami, FL, USA, November 12-16, 2024*. Association for Computational  
767 Linguistics, 2024.

768 Balázs Hidasi, Alexandros Karatzoglou, Linas Baltrunas, and Domonkos Tikk. Session-based  
769 recommendations with recurrent neural networks. In *ICLR*, 2016.

770 Jiaxi Tang and Ke Wang. Personalized top-n sequential recommendation via convolutional sequence  
771 embedding. In *WSDM*, 2018.

772 Wang-Cheng Kang and Julian J. McAuley. Self-attentive sequential recommendation. In *ICDM*,  
773 2018.

774 Hangzhan Jin, Sicheng Lv, Sifan Wu, and Mohammad Hamdaqa. RL is neither a panacea nor a  
775 mirage: Understanding supervised vs. reinforcement learning fine-tuning for llms, 2025. URL  
776 <https://arxiv.org/abs/2508.16546>.

777 Zhoujun Cheng, Shibo Hao, Tianyang Liu, Fan Zhou, Yutao Xie, Feng Yao, Yuexin Bian, Yonghao  
778 Zhuang, Nilabjo Dey, Yuheng Zha, Yi Gu, Kun Zhou, Yuqi Wang, Yuan Li, Richard Fan, Jian-  
779 shu She, Chengqian Gao, Abulhair Saparov, Haonan Li, Taylor W. Killian, Mikhail Yurochkin,  
780 Zhengzhong Liu, Eric P. Xing, and Zhiting Hu. Revisiting reinforcement learning for LLM  
781 reasoning from A cross-domain perspective. *CoRR*, abs/2506.14965, 2025.

782 Chao Feng, Wuchao Li, Defu Lian, Zheng Liu, and Enhong Chen. Recommender forest for efficient  
783 retrieval. In *Advances in Neural Information Processing Systems 35: Annual Conference on Neural  
784 Information Processing Systems 2022, NeurIPS 2022, New Orleans, LA, USA, November 28 -  
785 December 9, 2022*, 2022.

786 Ye Wang, Jiahao Xun, Minjie Hong, Jieming Zhu, Tao Jin, Wang Lin, Haoyuan Li, Linjun Li, Yan  
787 Xia, Zhou Zhao, and Zhenhua Dong. EAGER: two-stream generative recommender with behavior-  
788 semantic collaboration. In *Proceedings of the 30th ACM SIGKDD Conference on Knowledge  
789 Discovery and Data Mining, KDD 2024, Barcelona, Spain, August 25-29, 2024*, pages 3245–3254.  
790 ACM, 2024.

791 Leslie Pack Kaelbling, Michael L. Littman, and Andrew W. Moore. Reinforcement learning: A  
792 survey. *J. Artif. Intell. Res.*, 1996.

793 Richard S. Sutton and Andrew G. Barto. *Reinforcement learning - an introduction*, 2nd Edition. MIT  
794 Press, 2018.

795 John Schulman, Filip Wolski, Prafulla Dhariwal, Alec Radford, and Oleg Klimov. Proximal policy  
796 optimization algorithms. *CoRR*, 2017.

797 Timo Kaufmann, Paul Weng, Viktor Bengs, and Eyke Hüllermeier. A survey of reinforcement  
798 learning from human feedback. *CoRR*, 2023.

799 Rafael Rafailov, Archit Sharma, Eric Mitchell, Christopher D. Manning, Stefano Ermon, and Chelsea  
800 Finn. Direct preference optimization: Your language model is secretly a reward model. In  
801 *Advances in Neural Information Processing Systems 36: Annual Conference on Neural Information  
802 Processing Systems 2023, NeurIPS 2023, New Orleans, LA, USA, December 10 - 16, 2023*, 2023.

803 Rosie Zhao, Alexandru Meterez, Sham M. Kakade, Cengiz Pehlevan, Samy Jelassi, and Eran Malach.  
804 Echo chamber: RL post-training amplifies behaviors learned in pretraining. *CoRR*, abs/2504.07912,  
805 2025.

---

810 Victor Sanh, Albert Webson, Colin Raffel, Stephen H. Bach, Lintang Sutawika, Zaid Alyafeai,  
811 Antoine Chaffin, Arnaud Stiegler, Arun Raja, Manan Dey, M Saiful Bari, Canwen Xu, Urmish  
812 Thakker, Shanya Sharma Sharma, Eliza Szczechla, Taewoon Kim, Gunjan Chhablani, Nihal V.  
813 Nayak, Debajyoti Datta, Jonathan Chang, Mike Tian-Jian Jiang, Han Wang, Matteo Manica,  
814 Sheng Shen, Zheng Xin Yong, Harshit Pandey, Rachel Bawden, Thomas Wang, Trishala Neeraj,  
815 Jos Rozen, Abheesht Sharma, Andrea Santilli, Thibault Févry, Jason Alan Fries, Ryan Teehan,  
816 Teven Le Scao, Stella Biderman, Leo Gao, Thomas Wolf, and Alexander M. Rush. Multitask  
817 prompted training enables zero-shot task generalization. In *ICLR*, 2022.

818 An Yang, Baosong Yang, Beichen Zhang, Binyuan Hui, Bo Zheng, Bowen Yu, Chengyuan Li,  
819 Dayiheng Liu, Fei Huang, Haoran Wei, Huan Lin, Jian Yang, Jianhong Tu, Jianwei Zhang, Jianxin  
820 Yang, Jiaxi Yang, Jingren Zhou, Junyang Lin, Kai Dang, Keming Lu, Keqin Bao, Kexin Yang,  
821 Le Yu, Mei Li, Mingfeng Xue, Pei Zhang, Qin Zhu, Rui Men, Runji Lin, Tianhao Li, Tingyu Xia,  
822 Xingzhang Ren, Xuancheng Ren, Yang Fan, Yang Su, Yichang Zhang, Yu Wan, Yuqiong Liu, Zeyu  
823 Cui, Zhenru Zhang, and Zihan Qiu. Qwen2.5 technical report. *CoRR*, 2024.

824  
825  
826  
827  
828  
829  
830  
831  
832  
833  
834  
835  
836  
837  
838  
839  
840  
841  
842  
843  
844  
845  
846  
847  
848  
849  
850  
851  
852  
853  
854  
855  
856  
857  
858  
859  
860  
861  
862  
863

---

864    **A RELATED WORK**  
865  
866  
867

868    **A.1 GENERATIVE RECOMMENDATION**  
869  
870

871    In recent years, generative recommendation has attracted considerable attention in both academia  
872    and industry. This emerging paradigm, usually built on the Transformer architecture, reformulates  
873    recommendation as an end-to-end next-item generation task and thereby raises the performance ceiling  
874    of recommender systems. Early work TIGER (Rajput et al., 2023) employs residual quantization  
875    (RQ-VAE) (Zeghidour et al., 2022) to convert text embeddings—extracted from an item’s title and  
876    description—into discrete semantic IDs, which are then used for next-item prediction. HSTU (Zhai  
877    et al., 2024) propose a new architecture designed for high cardinality, non-stationary streaming  
878    recommendation data. LC-Rec (Zheng et al., 2024) aligns an LLM with semantic IDs via multi-task  
879    learning, enabling the model to “understand” the IDs and perform generative recommendation. Other  
880    studies investigate how to build better semantic IDs to enhance generation quality: RecForest (Feng  
881    et al., 2022) applies hierarchical k-means clustering and treats the cluster indices as tokens, while  
882    EAGER (Wang et al., 2024) and TokenRec (Qu et al., 2024) integrate semantic and collaborative  
883    signals directly into the tokenizer.

884    Very recently, generative recommendation has been rolled out at an industrial scale to address the  
885    drawbacks of traditional cascade systems. MTGR (Wang et al., 2025a) keeps the original deep  
886    learning recommendation model (DLRM) features, introduces user-level compression, and speeds  
887    up both training and inference for large-scale deployment. OneRec (Deng et al., 2025) lowers the  
888    serving cost with a Lazy Decoder-Only Architecture and stabilises training through an improved  
889    reinforcement learning algorithm.

890    **A.2 LLM AND RL**  
891  
892

893    Reinforcement learning (RL) trains an agent through repeated interaction with an environment so  
894    as to maximise cumulative return (Kaelbling et al., 1996; Sutton and Barto, 2018). Within large-  
895    language-model (LLM) fine-tuning, RL with Human Feedback (RLHF) has become the de-facto  
896    recipe: it usually adopts Proximal Policy Optimisation (PPO) (Schulman et al., 2017) to align  
897    model behaviours with human preferences (Kaufmann et al., 2023). Unfortunately, PPO is memory-  
898    hungry at the billion-parameter scale, motivating a series of lighter alternatives. Direct Preference  
899    Optimisation (DPO) (Rafailov et al., 2023) removes the value network and directly maximises the  
900    log-likelihood gap between preferred and dispreferred outputs; s-DPO (Chen et al., 2024) adapts this  
901    idea to recommendation by casting softmax negative mining as a pairwise-preference signal. Yet,  
902    preference-based methods remain off-policy and often plateau below on-line RL. Group-Relative  
903    Policy Optimisation (GRPO) (Shao et al., 2024) mitigates memory cost by normalising rewards inside  
904    a small group of roll-outs and replaces a learned reward model with rule-based heuristics, achieving  
905    strong gains on reasoning-heavy tasks such as mathematics and programming (DeepSeek-AI et al.,  
906    2025; OpenAI et al., 2024).

907    Recent studies have begun to explore how SFT and RL jointly shape LLMs for generative recom-  
908    mendation. (Yoshihara et al., 2025) argues that the two stages are complementary: a prolonged  
909    SFT phase first pushes accuracy to its limit, after which on-line RL with GRPO further compresses  
910    the token budget at inference time. (Jin et al., 2025) shows that RL can largely recover the out-of-  
911    distribution accuracy lost during SFT by cancelling the directional drift of singular vectors rather than  
912    by discovering entirely new solutions. In contrast, (Yue et al., 2025) points out that the reasoning  
913    ability obtained through RL with verifiable rewards (RLVR) is bounded by the base model, whereas  
914    SFT can introduce genuinely new reasoning patterns, suggesting the need for more powerful RL  
915    paradigms such as continual scaling. (Cheng et al., 2025) adds a domain perspective: areas frequently  
916    encountered during pre-training (e.g., mathematics and code) profit from cross-domain RL, while  
917    low-exposure domains (e.g., logic and simulation) require in-domain RL for meaningful gains. (Zhao  
918    et al., 2025) observes that popular RL algorithms tend to converge to a single dominant output distri-  
919    bution, amplifying patterns already present in the pre-training data, yet they still display cross-task  
920    generalization.

918  
919  
920  
921  
922  
923  
924  
925

Input:  
The user has interacted with items <a\_13><b\_197><c\_1>, <a\_52><b\_17><c\_113>, <a\_13><b\_201><c\_34> in  
chronological order. Can you predict the next possible item that the user may expect?  
Response:  
<a\_13><b\_72><c\_149>

926  
927  
928  
929  
930  
931  
932  
933  
934

Figure 5: Semantic task prompt.

Input:  
What is the title of <a\_24><b\_141><c\_73>?  
Response:  
Oral-B Deep Sweep Toothbrush

932  
933  
934

Figure 6: Alignment task prompt1.

## B EXPERIMENTAL SETTINGS

935  
936  
937  
938  
939  
940  
941  
942

All conventional recommender baselines are optimized with binary cross-entropy (BCE) loss and the Adam optimizer. The learning rate is selected from  $\{1 \times 10^{-2}, 1 \times 10^{-3}, 1 \times 10^{-4}\}$ , while the weight-decay coefficient is tuned within  $\{1 \times 10^{-2}, 1 \times 10^{-3}, 1 \times 10^{-4}, 1 \times 10^{-5}, 1 \times 10^{-6}\}$ . A mini-batch size of 1024 is used throughout. For TIGER, we adopt T5 (Sanh et al., 2022) as the encoder-decoder backbone and use Qwen3-Embedding-4B to generate item embedding. Every LLM-based method, including ours, is built upon Qwen2.5-Instruct-0.5B (Yang et al., 2024) to keep the computational footprint modest, and is trained with the AdamW optimizer.

943  
944  
945  
946  
947

The SFT and preference-alignment data are processed in batches of 128, whereas RL batches contain 512 samples. We set the learning rate to  $3 \times 10^{-4}$  for SFT and to  $1 \times 10^{-5}$  for both S-DPO and SINGER, together with a cosine decay scheduler. SFT runs for ten epochs with early stopping (patience = 1). S-DPO is trained for a single epoch, and we fix  $\beta = 0.1$  and sample three negative items. For D<sup>3</sup>, the interpolation coefficient  $\alpha$  is chosen from  $\{0.8, 0.9, 1.0\}$ .

948  
949  
950  
951  
952  
953  
954  
955  
956  
957  
958  
959  
960

For the SID generation stage of SINGER, we utilize Qwen3-Embedding-4B as the text encoder to transform item titles and descriptions into their corresponding embeddings. The tokenizer is trained on 8 GPUs with a per-device batch size of 2048. RQ-VAE is trained layer-wise for 1 000 steps per layer, with a learning rate of  $1 \times 10^{-3}$ . We employ a Constrained Balanced RQ-KMeans algorithm to generate SIDs. Specifically, we perform residual quantization layer-wise with a codebook size of  $K = 256$ . To prevent cluster collapse and maximize codebook utilization, we enforce strict size constraints on each cluster, ensuring a balanced tree structure. The clustering is optimized for a maximum of 100 iterations per layer with a convergence tolerance of  $1 \times 10^{-7}$ . Crucially, to ensure a strictly one-to-one mapping between items and SIDs, we apply a deterministic deduplication step: for any items sharing the same semantic path, a unique suffix token is appended to resolve conflicts. Following SID generation, the SFT stage is conducted with a batch size of 128 for up to ten epochs (early stopping, patience = 1), followed by the full-process alignment-guided RL for two epoch under the same  $\beta$  and candidate settings as described above.

961  
962

## C DATASETS

963  
964  
965

We evaluate our approach on two subsets of the Amazon Review corpus: *Industrial\_and\_Scientific* and *Office\_Products*. To keep the computational cost manageable, we adopt a data-reduction procedure

966  
967  
968  
969  
970  
971

Input:  
Which item has the title Nashua Stretch & Seal Self-Fusing Silicone Tape?  
Response:  
<a\_202><b\_202><c\_29>

Figure 7: Alignment task prompt2.

972

973

Input:

The user has interacted with items 'Kreg SML-C150-100 Pocket Screws 1-1/2-Inch, 8 Coarse, Washer-Head, 100-Count', '3M Flap Disc 566A, T29, 4-1/2"" Diameter, 40 Grit, 5/8""-11 Thread (Pack of 1)' in chronological order. Can you predict the next possible item that the user may expect?

974

975

Response:

<a\_104><b\_60><c\_152>

976

977

978

979

980

Figure 8: Alignment task prompt3.

981

Input:

The user has interacted with items '<a\_71><b\_44><c\_249>', '<a\_71><b\_114><c\_136>', '<a\_67><b\_244><c\_35>' in chronological order. Can you predict the title of the next item that the user may expect?

982

983

Response:

Install Bay Copper Ring Terminal Connector 8 Gauge 5/16 Inch 25 Pack - CUR8516]", J-B Weld 8265S Original Cold-Weld Steel Reinforced Epoxy - 2 oz.

984

985

986

987

988

989

Figure 9: Alignment task prompt4.

990

991

992

993

994

995

inspired by the strategy in (Bao et al., 2024). The preprocessing steps are as follows: (1) users and items with fewer than five interactions are removed; (2) for the *Toys\_and\_Games* subset, only records from October 2016 to November 2018 are retained; (3) for the smaller *Industrial\_and\_Scientific* subset, we keep all interactions between October 1996 and November 2018; (4) each user's interaction sequence is truncated to a maximum length of ten; (5) finally, each dataset is split chronologically into training, validation, and test partitions with an 8:1:1 ratio. The main statistics of the resulting training splits are listed in Table 3.

996

997

998

999

1000

Table 3: Statistics of datasets.

1001

1002

1003

1004

Datasets	Industrial	Office
Items	3,685	3,459
Train	3,6259	3,8924
Valid	4,532	4,866
Test	4,533	4,866

1005

1006

1007

## D ALIGNMENT PROMPTS

1008

1009

For the semantic task, a sample prompt is shown in the Figure 5.

1010

1011

Representative examples for the alignment tasks are presented in Figures 7, 6, 8, 9, and 10.

1012

1013

## E LIMITATION

1014

1015

1016

1017

1018

1019

1020

1021

1022

1023

1024

1025

Input:

An item can be described as follows: Tach-It B-1 single-edge industrial razor blades (pack of 100) are high-carbon steel replacement blades designed for heavy-duty cutting and scraping tasks; they fit most standard single-edge blade holders and come packaged in a convenient bulk dispenser. Which item is it describing?

Response:

<a\_17><b\_91><c\_139>

Figure 10: Alignment task prompt5.

---

1026 SINGER’s performance remains unclear. Second, despite its potential, we did not investigate how  
1027 to systematically improve the cross-domain performance of the SINGER-w/o-SFT variant. These  
1028 limitations indicate that future work should explore the scalability and robustness of SINGER in  
1029 more resource-intensive and iterative settings, thereby offering a more comprehensive assessment of  
1030 its practical usefulness.

1031

## 1032 F LLM USAGE

1033

1034 LLMs were employed exclusively for linguistic polishing and stylistic refinement of the manuscript.  
1035 No LLM was used to generate experimental designs, implement algorithms, produce empirical results,  
1036 or analyze data. All technical contributions, including model architecture, training protocol, and  
1037 evaluation pipeline, were conceived, implemented, and verified by the authors themselves.

1038

1039

1040

1041

1042

1043

1044

1045

1046

1047

1048

1049

1050

1051

1052

1053

1054

1055

1056

1057

1058

1059

1060

1061

1062

1063

1064

1065

1066

1067

1068

1069

1070

1071

1072

1073

1074

1075

1076

1077

1078

1079